HUNTINGTON MEDICAL RESEARCH INSTITUTES

NEUROLOGICAL RESEARCH LABORATORY

734 Fairmount Avenue

Pasadena, California 91105

Contract No. NO1-NS-5-2324

QUARTERLY PROGRESS REPORT

April 1 - June 30, 1997

Report No. 10

"SAFE AND EFFECTIVE STIMULATION OF NEURAL TISSUE"

William F. Agnew, Ph.D.

Ted G.H. Yuen, Ph.D.

Douglas B. McCreery, Ph.D.

Randy R. Carter, Ph.D.

Leo A. Bullara, B.A.

Albert S. Lossinsky, Ph.D.

1

This QPR is being sent to
you before it has been
reviewed by the staff of the
Neural Prosthesis Program.

ABSTRACT

During the past quarter we have implanted arrays of 7 activated-iridium microelectrodes into the left postcruciate gyrus of 7 adult cats. The histologic results of these studies are presented in this report and the physiologic findings (pyramidal tract evoked potentials and multiunit recordings taken from the stimulating electrodes) will be reported in the October QPR. In this series of animals, we observed a marked decrease in the numbers of micro-hemorrhages, cavitations and insertion trauma which we attribute to changes in the surgical technique and electrode configuration and to a reduction in the thickness of the electrode shaft. In this study we focused mainly on the mechanism of induction of large lymphocytic aggregations at the tips of the pulsed electrodes. This and other problems presented by the use of microstimulation in CNS neural prostheses are discussed.

INTRODUCTION

This report describes our continuing investigations of the limits of safe microstimulation of neurons in the cat sensorimotor cortex and also further investigations into the mechanisms underlying neural damage that may result from implantation, long-term residence and pulsing of these electrodes in nervous tissue. In this study, we report the results of chronic experiments on seven cats implanted with arrays of seven activated iridium microelectrode, in which we have focused on determining the relationship of stimulus parameters and neural damage as well as the phenomenon of lymphocytic accumulation at the tip of pulsed microelectrodes.

METHODS

Microelectrodes. The intracortical arrays contain 7 discrete activated iridium microelectrodes extending from a button of Hysol epoxy, approximately 2.5 mm in diameter. The microelectrode shafts are spaced 380 µm apart center to center. The shaft in the center of the cluster is 2 mm in length. Three of the shafts are 1.5 mm in length, and three are 1.7 mm in length. In the first part of this series (prior to animal IC-153), the iridium shafts were 50 µm in diameter before application of the Epoxylite insulation. In subsequent animals, they were 32-37 µm. The conical tips of the microelectrodes are quite blunt, with radii of curvature of 5-6 µm. The geometric area of the exposed tips is 450 µm², ± 10%. The arrays are integrated with a 16-pin percutaneous connector that also includes a large indifferent platinum electrode, a Ag/AgCl reference electrode and connections for the pyramidal tract recording electrode and reference electrode. The complete assembly is soaked in deionized water for 48 hours, then sterilized with ethylene oxide.

Surgical Procedure. The arrays were implanted into seven young adult cats of either sex, using general anesthesia and aseptic surgical technique. The animal's head was mounted in a stereotaxic holder, the scalp and muscles were reflected in a

midline incision, and the pericruciate gyri (sensorimotor cortex) exposed. The frontal air sinus was partly filled with cranioplasty. The percutaneous connector was mounted to the skull with stainless steel screws and methacrylate bone cement. A macrostimulating electrode was placed on the dura over the postcruciate gyrus, and a recording electrode was implanted into the pyramidal tract through a small burr hole over the cerebellum. The large pyramidal tract potential evoked from the surface of the postcruciate gyrus was used to guide the recording electrode into the tract. The recording electrode was then sealed to the skull using methacrylate bone cement.

A small flap, slightly larger than the array's superstructure, was made in the dura over the postcruciate cortex, and the array of microelectrodes was inserted manually into the cortex by grasping its cable with padded forceps while pushing the array into the brain. In this series of animals, we did not suture the dura over the array, but in recent animals (IC-161 and thereafter, Table 1), we covered the array with a sheet of perforated artificial dura (silastic sheeting). The cortex was then covered with gelfoam and the skull defect sealed with cranioplasty.

At least 45 days after implantation, the 7-hour test stimulation regimen was conducted, with the animal lightly anesthetized with Propofol. Before and after the test stimulation, the response evoked by the intracortical microelectrodes was recorded from the pyramidal tract. By this method, we have determined that the Propofol anesthesia does not reduce the amount of neural activity evoked by the microelectrodes, and that it does not induce an elevation of the electrical threshold of the cortical neurons. The stimulation regimens were 7 hours in duration. The electrodes were pulsed continuously with charge-balanced, controlled-current, cathodic-first pulses. The pulse duration was 400 μsec/ph in most instances (150 μsec/ph in animal IC-161). In most animals, 5 microelectrodes were pulsed and two were left as unpulsed controls (except in IC-149 in which all seven were pulsed). To assess the role of "mass action" on neural damage and/or the lymphocytic accumulation, only one electrode was pulsed in IC-150 and only 2 of 7 in IC-162. In most animals, the microelectrodes were pulsed simultaneously, but they were pulsed in

4

the interleaved mode in animals IC-158 and IC-161. The stimulus parameters for each animal are listed in Table 1 below.

Table 1

Animal IC #	Stim.date	Post-implant (Days)	No. Electrodes pulsed	Mode	Freq. (Hz)	I (µA)	Charge/ph (nC)	Pulse Duration (µsec)	Shaft Diameter (µm)
149	3/6/97	87	(7)1,2,3,4,5,6,7	simult	200	20	8	400	50
150	7/8/97	140	(1)7	-	200	20	8	400	50
153	4/4/97	45	(5)2,3,4,5,7	simult	200	20	8	400	35
156	6/17/97	90	(5)2,3,4,5,6	simult	50	20	8	400	35
158	6/18/97	77	(5) 1,4,5,6,7	interlv	200	20	8	400	35
161	7/22/97	50	(5),1,3,4,5,6	interlv	200	53	8	150	35
162	8/8/97	58	(2) 4, 7	simult	200	20,10	8,4	400	35

Within 45 minutes after the end of the stimulation, the cats were anesthetized with Nembutal and perfused through the ascending aorta with ½ strength Karnovsky's fixative (animal IC-158 was perfused with buffered paraformaldehyde fixative).

Histologic evaluations were carried out on serial 8 µm thick paraffin sections cut in the horizontal plane (perpendicular to the electrode shafts). The sections included both pulsed (left) and unpulsed (right) cruciate gyri. While we considered the evaluation of the tissue at the pulsed tips to be most critical, serial sections enabled observation of histologic alterations along the entire shaft. At 100 µm intervals below the pial surface, we recorded the presence of any inflammatory cells, hemorrhage, cavitation, scarring, gliosis, edema, sheath thickness, as well as the condition of the neurons, the appearance of blood vessels in the area at these levels.

RESULTS

Gross appearance of implant sites. Figure 1 shows the typical post-perfusion appearance of the 7-iridium microelectrode array, including a short length of the cable in situ on the left postcruciate gyrus. In most cases the Hysol disk (electrode matrix)

5

the array was relatively level with the pial surface as shown in Fig. 1. After removal of the array there was usually a shallow cortical impression of the array matrix. The entry sites of the 7 electrodes were usually visible with a dissecting microscope and in all cases appeared free of hemorrhage or infection.

Microscopic findings. All evaluations were conducted by one of us (TGHY) without knowledge of which electrodes had been pulsed. Table 2 presents a representative, detailed histology report for one animal (IC-153) which demonstrates the extensive analysis required for a complete evaluation of each of the 7 electrode tracks through their complete traverse in the cerebral cortex from the pial surface to the tips. Table 3 presents a summary of the results taken from the more detailed reports illustrated by Table 2. Representative horizontal sections taken through the electrode tracks of the array shown in Fig. 1 are visible in a hexagonal pattern at a depth of 300 μm in Figures 2 and 3. The connective tissue sheath surrounding the tracks was very thin (generally 3-8 μm). With few exceptions, there were no hemorrhages, cavitations or glial scars in any of the cats. When such changes were present, they were small and appeared inconsequential.

Gliosis. In most cases, gliosis was very sparse at the electrode tips with no instance of gliotic scarring at the tips or along the shafts of the microelectrodes. However, there was a marked gliosis surrounding the shafts of 11 of 49 of the electrodes (Figs. 4-6). This gliosis consisted of clusters of tightly-packed astrocytes along the shafts at levels as shallow as 70 μm below the pial surface and as deep as 700 μm below the pia. These gliotic clusters were never adjacent to all the electrodes in any one array. Their frequency ranged from none of the 7 microelectrodes (3 animals) to 5 of the 7 microelectrodes (1 animal). Since the gliosis always occurred on the epoxy-insulated shaft of both pulsed and unpulsed electrodes, there was no correlation with current flow.

Neurons. In six of the seven animals, a few neurons along the shaft, as well as at the tip, were slightly flattened, probably as a result of tissue displacement by the electrode (Fig. 7). In one animal (IC-161), there appeared to be patches of poorly fixed

cortex with several stellate, hyperchromic neurons in the vicinity of, and remote from, pulsed and unpulsed electrodes. There were occasional instances of edema surrounding the track of the shaft (Fig. 8). In cases in which the tips of electrodes were surrounded by a sphere of packed lymphocytes (discussed below) up to 200 μm in diameter, the exact state of the neurons within this mass was obscured. Evidence of displacement of neurons into the surrounding neuropil was not observed.

Lymphocytic aggregation. The predominant histologic feature in this series of animals was the occurrence of large numbers of lymphocytes, densely aggregated at the microelectrode tips, and especially at the tips of pulsed microelectrodes. In all cases in which more than 100 lymphocytes were present in a histologic section (+++), the electrodes had been pulsed at 8 nC. Lymphocytes around unpulsed electrodes never exceeded (+). The aggregates extended approximately 100-300 μm above and below the tip (Table 2, Electrodes #2-5, Table 3, Figs. 9-10). All pulsed electrodes, with two exceptions, were pulsed at 200 Hz, 20 μA, pulse durations of 400 μsec (8 nC/ph) and pulsed in a continuous, simultaneous mode. The microelectrodes in animals IC-158 and IC-161 were pulsed with the same parameters but in an interleaved mode and those in IC-156 were pulsed at 50 Hz. However, interleaved pulsing failed to prevent or significantly reduce the lymphocytic aggregation. Similarly, reducing the frequency to 50 Hz did not reduce the size of the aggregates. In animals IC-150 and IC-162, only one and two, respectively, of the 7 electrodes were pulsed. In both cases, there were aggregates of lymphocytes at the tips of the pulsed microelectrodes.

At the sites of the lymphocytic aggregates, nearby blood vessels showed marked perivascular cuffing and often there was streaming of lymphocytes toward an adjacent pulsed electrode (Fig. 11). In one instance, the emigration of lymphocytes was unable to penetrate a thick cluster of glial cells ensheathing the shaft of the microelectrode a short distance from the tip (Fig. 12)

7

TABLE 2

SUMMARY OF HISTOLOGIC FINDINGS
FROM ONE ANIMAL (IC-153)

ELEC-TRODE	DEPTH (µm)	INFLAMM	HEMORR	CAVITAT SIZE (µm)	SCAR	GLIO-SIS	NEURONS	EDEMA	SHEATH THICKNESS (µm)	LYMPHO-CYTES	VASC	COMMENTS
1	Surface	0	0	0	0	++	NA	0	5	0	0	
	100	0	0	25× 60	0		Occas. Flat	0	3-15	0	N	
	200	0	0	0	0	0	N	0	2-13	0	N	
	300	0	0	0	0	0	N	0	3-8	0	N	
	400	0	0	0	0	0	N	0	3	0	N	
	500	0	0	0	0	0	N	0	5	0	N	
	600	0	0	0	0	0	N	0	3-5	0	N	Ly. in nearby vessel
	700	0	0	0	0	+	N	0	5	0	+ Hyper-trophy	
	800	0	0	0	0	+	N	0	3	+	N	
	900	0	0	0	0	+	-	0	5	0	N	
	910	0	0	0	0	0	-	0	—	+	+ Hyper-plasia	Numerous Ly. in nearby vessels
	Tip 930	0	0	0	0	0	N	0	3	0	N	
2	Surface	0	0	0	0	0		0	2—8	0	N	
	100	0	0	0	0	0 ·	N	0	3-5	0	N	
	200	0	0	0	0	0	Occas. Flat	0	2-5	0	N	
	300	0	0	0	0	0	N	0	5	0	N	
	400	0	0	0	0	0	N	0	3	0	N	
	500	0	0	0	0	0	N	0	5	0	N	
	600	0	0	0	0	0	N	0	5	0	N	Ly. cuffing in nearby vessels
	650	0	0	0	0	0	Occas. Flat	0	5	+++	N	
	Tip 680	0	0	0	0	0	Occas. Flat	0	—	+++	N	Ly. cuffing in nearby vessels
	700	0	0	0	0	0	Occas. Flat	0	—	+++	+ Hyper-trophic	Ly. cuffing in nearby vessels
	760	0	0	0	0	0	N	0	—	+++	++ Hyper-trophic	

N = Normal
NA = Not Applicable

GLIOSIS CODE
\+ Mild
++ Moderate
+++ Marked

LYMPHOCYTE CODE
\+ = <50 in histologic section
++ = 50-100 "
+++ = >100 "

Ly = Lymphocytes

TABLE 2 (CONT.)

ELEC-TRODE	DEPTH (µm)	INFLAMM	HEMORR	CAVITAT. SIZE (µm)	SCAR	GLIO-SIS	NEURONS	EDEMA	SHEATH THICKNESS (µm)	LYMPHO-CYTES	VASC	COMMENTS
3	Surface	0	0	0	0	0	NA	0	5-8	0	N	
	100	0	0	13× 25	0	0	N	0	3	0	N	Occas. Ly. in nearby vessels
	200	0	0	0	0	0	Occas. Flat	0	3-8	0	N	
	300	0	0	0	0	0	N	0	5-10	0	N	Occas. Ly. In 3 nearby vessels
	400	0	0	0	0	0	Occas. Flat	0	3	0	N	
	500	0	0	0	0	0	N	0	3	0	N	Occas. Ly. In nearby vessels
	600	0	0	0	0	0	N	0	3	+	N	
	700	0	0	0	0	0	N	0	5	+	+ Hyper-trophic	Ly. in nearby vessels
	800	0	0	0	0	++	Occas. Flat	0	--	+++	N	
	850	0	0	0	0	0	Occas. Flat	0	--	+++	++ Hyper-trophic	
	Tip 870	0	0	0	0	0	N	0	--	+++	N	
	900	0	0	0	0	0		0	--	++		
	910	0	0	0	0	0	N	0	--	++	N	
4	Surface	0	0	0	0	0	NA	0	3	0	N	
	100	0	0	0	0	0	N	0	3-13	0	N	
	200	0	0	0	0	0	Occas. Flat	0	3-8	0	N	
	300	0	0	0	0	0	N	0	3-10	0	N	
	400	0	0	0	0	0	N	0	5	0	N	Occas. Ly. in nearby vessel
	500	0	0	0	0	0	N	0	5	0	N	
	600	0	0	0	0	0	Occas. Flat	0	5	+	N	
	Tip 700	0	0	0	0	+	Occas. Flat	0	--	+++	N	
	750	0	0	0	0	N	N	0	--	++	N	
5	Surface	0	0	0	0	+	NA	0	3	0	N	
	100	0	0	0	0	+	N	0	5-8	0	N	
	200	0	0	0	0	+	Occas. Flat	0	5-8	0	N	
	300	0	0	0	0	0	N	0	3-10	0	N	
	400	0	0	0	0	0	N	0	3	+	N	Occas. Ly. in nearby vessel
	500	0	0	0	0	0	N	0	5	0	N	

TABLE 2 (CONT.)

ELEC-TRODE	DEPTH (µm)	ACUTE INFLAMM	HEMORR	CAVITAT. SIZE (µm)	SCAR	GLIO-SIS	NEURONS	EDEMA	SHEATH THICKNESS (µm)	LYMPHO-CYTES	VASC	COMMENTS
5 (cont.)	600	0	0	0	0	0	Occas. Flat	0	5	0	N	
	700	0	0	0	0	++	N	0	5	++	N	
	800	0	0	0	0	0	Occas. Flat	0	3	+++	++ Hyper-plasia	
	900	0	0	0	0	0	N	0	--	+++	++ Hyper-plasia	
	Tip 920	0	0	0	0	0	N	0	--	+++	N	
	960	0	0	0	0	0		0	--	+	N	
6	Surface	0	0	0	0	0	Occas. Flat	0	5-8	0	N	
	100	0	0	0	0	0	Occas. Flat	0	3-5	0	N	
	200	0	0	0	0	0	N	0	2-5	0	N	
	300	0	0	0	0	+	N	0	2-8	0	N	
	400	0	0	0	0	0	Occas. Flat	0	2-10	0	N	
	500	0	0	0	0	0	N	0	5	0	N	
	600	0	0	0	0	++	Occas. Flat	0	--	0	N	
	Tip 610	0	0	0	0	0	? Masson's Stain	0	--	+	N	
	640	0	0	0	0	0	N	0	--	+	N	
7	Surface	0	0	0	0	+	Occas. Flat	0	3-5	0	+ Hyper-plasia	
	100	0	0	0	0	+	N	0	5-8	0	N	
	200	0	0	? 40 × 50	0	0	Occas. Flat	0	2-5	0	N	
	300	0	0	10 × 60	0	0	N	0	3-5	0	N	
	400	0	0	0	0	++	Occas. Flat	0	5	0	N	
	500	0	0	0	0	+	N	0	10	0	++ Hyper-plasia	Several Ly. in nearby vessel.
	600	0	0	0	0	+	N	0	3-8	0	N	Several Ly. in nearby vessel.
	700	0	0	0	0	++	N	0	8	0	N	
	800	0	0	0	0	0	Occas. Flat	0	5	+	+ Hyper-tro.	Ly. in nearby vessels.
	850	0	0	0	0	0	--	0	8	++	++ Hyper-tro.	
	900	0	0	0	0	0	--	0	—	+++	+ Hyper-plasia	Numerous Ly. in nearby vessels
	Tip 950	0	0	0	0	0	N	0	--	+++	N	
	980	0	0	0	0	0	Occas. Flat	0	--	++	N	

N = Normal
NA = Not Applicable

GLIOSIS CODE
+ Mild
++ Moderate
+++ Marked

LYMPHOCYTE CODE
+ = <50 in histologic section
++ = 50-100 "
+++ = >100 "

Ly = Lymphocytes

TABLE 3
HISTOLOGIC RESULTS OF PULSED AND UNPULSED MICROELECTRODE ARRAYS

UNPULSED

IC #		1	2	3	4	5	6	7
149	ELECTR. #	–	–	–	–	–	–	–
	Edema							
	Gliosis							
	Neurons							
	Lymphocytes							
150	ELECTR. #	1	2	3	4	5	6	–
	Edema	0	0	0	0	0	0	
	Gliosis	+	++	+	0	0	+	
	Neurons	N	N	NA	NA	N	N	
	Lymphocytes	0	0	0	0	0	0	
153	ELECTR. #	1	–	–	–	–	6	–
	Edema	0					0	
	Gliosis	0					0	
	Neurons	N					N	
	Lymphocytes	0					+	

PULSED

IC #		1	2	3	4	5	6	7
149	ELECTR. #	1	2	3	4	5	6	–
	Edema	0	0	0	0	0	0	
	Gliosis	++	+	+	++	+	++	
	Neurons	Occ. Flat.	Occ. Flat.	Occ. Flat.	Occ. Flat.	N	N	
	Lymphocytes	+	+++	+++	+++	+++	+	
150	ELECTR. #	–	–	–	–	–	–	7
	Edema							
	Gliosis							
	Neurons							
	Lymphocytes							+++ at nearby vessels
153	ELECTR. #	–	2	3	4	5	–	7
	Edema		0	0	0	0		0
	Gliosis		0	0	0	0		0
	Neurons		N	N	N	?		+ Flat.
	Lymphocytes		+++	+++	++	+++		+++

TABLE 3 (CONT.)
HISTOLOGIC RESULTS OF PULSED AND UNPULSED MICROELECTRODE ARRAYS

IC # 156

UNPULSED

ELECTR.#	1	–	–	–	–	–	7
Edema	0						0
Gliosis	0						+
Neurons	NA						NA
Lymphocytes	0						+

PULSED

ELECTR.#	–	2	3	4	5	6	–
Edema		0	0	0	0	0	
Gliosis		0	0	0	+	+	
Neurons		Occ. Flat.	N	N	N	N Flat.	
Lymphocytes		+++	+++	++	++	+	

IC # 158

UNPULSED

ELECTR.#	–	2-	3-	–	–	–	–
Edema		0	0				
Gliosis		+	+				
Neurons		N	N				
Lymphocytes		+	0				

PULSED

ELECTR.#	1	2	3	4	5	6	7
Edema	0			0	0	0	0
Gliosis	+			+	0	0	+
Neurons	NA		0?	NA	N	++ Flat.	N
Lymphocytes	+	+	+++	+++	+++	+	+

IC # 161

UNPULSED

ELECTR.#	–	2	–	–	–	–	7
Edema		0					0
Gliosis		+					+
Neurons		N					+ Hyperchromic (Fixation art.)
Lymphocytes		+					++

PULSED

ELECTR.#	1	–	3	4	5	6	–
Edema	0		0	0	0	0	
Gliosis	0		+	+	0	+	
Neurons	N		Occ. Flat.	N	N	N	
Lymphocytes	++		+++	+	+++	+++	

IC # 162

UNPULSED

ELECTR.#	1	2	3	–	5	6	–
Edema	0	0	0		0	0	
Gliosis	0	0	0		0	0	
Neurons	N	occ. Flat	N		N	N	
Lymphocytes	0	+	0		0	0	

PULSED

ELECTR.#	1	–	–	4	–	–	7
Edema	0			0			0
Gliosis	+			+			+
Neurons	N: within Ly. Aggreg.			N: within Ly. Aggreg.			N: within Ly. Aggreg.
Lymphocytes	+++			+++			+++

N = Normal
NA = Not Applicable

GLIOSIS CODE
+ Mild
++ Moderate
+++ Marked

LYMPHOCYTE CODE
+ = <50 in histologic section through the site of the microelectrode tip
++ = 50-100 ""
+++ = >100 ""

Ly = Lymphocytes

DISCUSSION

The marked reduction in the trauma and microhemorrhages resulting from electrode insertion in this series is very encouraging and can be attributed to several factors. Firstly, surgical techniques have been improved, as described in Methods (omitting suturing of the dura, the use of artificial dura and Gelfoam, etc.). Also, changes have been made in the configuration of the conical electrode tip (increased to 12 μm diameter), and reduction of the electrode shaft size, from 50 to 35 μm in the last 5 animals, which, along with changes in the tip configuration, considerably lessens the disruption of small blood vessels.

The gliosis (clumping of astrocytic elements) around some of the electrode shafts was a surprising finding. This marked (+++) gliosis occurred in animals IC-149, IC-150 and IC-158 and was not present in the 4 remaining animals. The gliosis had not transformed into scars but remained as a tightly packed aggregate of astrocytes. Since the gliosis was present only around a few of the electrodes while others (even in the same array) were free of these cells, some type of contamination of some electrodes is suggested, perhaps during one of the steps of fabrication. In the future, we will perform portions of the electrode fabrication process in a clean room.   In this series we initiated studies to determine the mechanism of the lymphocytic aggregation by varying several parameters while keeping charge/ph constant. Lymphocytic accumulation was unaffected by interleaved (in place of simultaneous) pulsing of the microelectrodes, and was essentially unaffected by the stimulus frequency over the range of 50 to 200 Hz. Also, when only one or two electrodes (of 7) were pulsed, the aggregates were just as dense as when 5 electrodes were pulsed. Reducing the stimulus pulse duration to 150 μsec while maintaining the charge/ph at 8 nC, did not reduce the magnitude of the aggregates.

From the data presented in this report, it is still unclear whether the lymphocytic accumulation is due to a true electrotaxic phenomenon or whether the lymphocytes are

13

attracted to a substance (cytokine, etc.) released locally from metabolically-altered or damaged neurons, or to a substance produced electrochemically at, and leaching from, the electrode-electrolyte interface. The presence of a few lymphocytes around the tips of some unpulsed electrodes and the variability in the density of the aggregate around the pulsed electrodes, speaks against a purely electrotaxic explanation.

Several years ago, when we first began to implant intracortical microelectrodes, we would conduct the stimulation regimen at 10 or 12 days after implantation, and we frequently observed dense aggregates of inflammatory cells around the pulsed tips. Later, when we extended the post-surgical time to at least 21 days, very few lymphocytes were seen around the pulsed tips. In the current series the aggregates of inflammatory cells occurred around the tips of pulsed microelectrodes in the 7-microelectrode arrays that have been implanted for more than 40 days. We are uncertain why the problem has recurred. In the current series, we have been pulsing 5 of 7 closely-spaced microelectrodes in the array of 7, whereas in earlier series, the microelectrodes were implanted individually and were at least 1 mm apart. Otherwise, the duration of the stimulation regimens, the stimulus frequency, and the charge per phase are no greater than those that we have used previously in studies in which the aggregations did not occur. It is possible that the ongoing, low- level mechanical trauma associated with so many closely-spaced microelectrodes may act as a cofactor with the electrical stimulation to promote the influx of inflammatory cells from the circulation. Perivascular cuffing by lymphocytes is a prominent feature of the phenomenon. Perhaps the blood-brain barrier is slightly abnormal within the environs of the array, even before the stimulation begins. We can address this question in our ongoing studies by observing if the aggregations around the pulsed tips and the attendant perivascular cuffing by lymphocytes is more severe when there is a greater "background" of mechanically-induced injury. If the influx of inflammatory cells is related to the "background" mechanical injury, then improving the arrays and the procedures for inserting them and stabilizing them after implantation may reduce this stimulation-related phenomenon.

14

Some of the stimulus parameters used in this study exceed those necessary for proposed or extant neural prostheses utilizing microstimulation. In particular, the microelectrodes were pulsed continuously for 7 hours, at 50 to 200 Hz. However, the accumulation of lymphocytes around the pulsed electrodes is relevant to the design of safe microstimulation protocols. The primary concern is the fate of neurons within the approximately 200 μm diameter clusters of lymphocytes, i.e., the aggregates designated as +++ in Tables 2 and 3. In all cases, these microelectrodes had been pulsed at 8 nC/phase for 7 hours. In addition, macrophages are completely absent at the time of sacrifice (45 minutes after a 7-hour stimulation). Displacement of neurons from even a portion of the space occupied by the lymphocytic mass seems unlikely since there is no evidence of such a displacement outward into the surrounding neuropil, e.g., increased neuronal density at the periphery of the lymphocytic aggregate.

Many questions remain. What is the time course of the aggregation and dispersion of lymphocytes, macrophages and other cell types after cessation of stimulation? In our earlier studies mentioned above, in which we pulsed the microelectrodes 10 or 11 days after implantation and there were many lymphocytes, we did note that the cells had mostly dispersed by 48 hours after the end of the stimulation. This must be confirmed in additional animals. Also, to what extent has the neuronal population near the electrodes been lost or displaced? Are the neurons lysed by lysosomal enzymes during this period, and if so, why are macrophages completely absent? We have found that evoked potentials recorded from the pyramidal tract are greatly diminished after the stimulation period. Multi-unit recordings from the stimulating electrodes after the 7-hour stimulation were carried out in 3 animals. There was a decrease in the number of units recorded before and after stimulation in each case. In one animal (IC-162), three units were recorded before stimulation and none was present afterwards. these and other questions need to be addressed. In our next QPR we will report in more detail on the results of pyramidal tract evoked potentials and multiunit recordings taken from this series of animals.

15

WORK NEXT QUARTER

We will continue to investigate the mechanisms of electrically-induced changes at the tips of intracortical microelectrodes. These include the undesirable consequences of lymphocytic accumulation, disruption or loss of neurons, depression of neural excitability and decreases in the numbers of recorded units following high intensity (8 nC) stimulations. We will also report the results of evoked potentials from the pyramidal tract and multiunit recordings before and after stimulation, for the experiments for which histologic evaluations were presented in the present report.
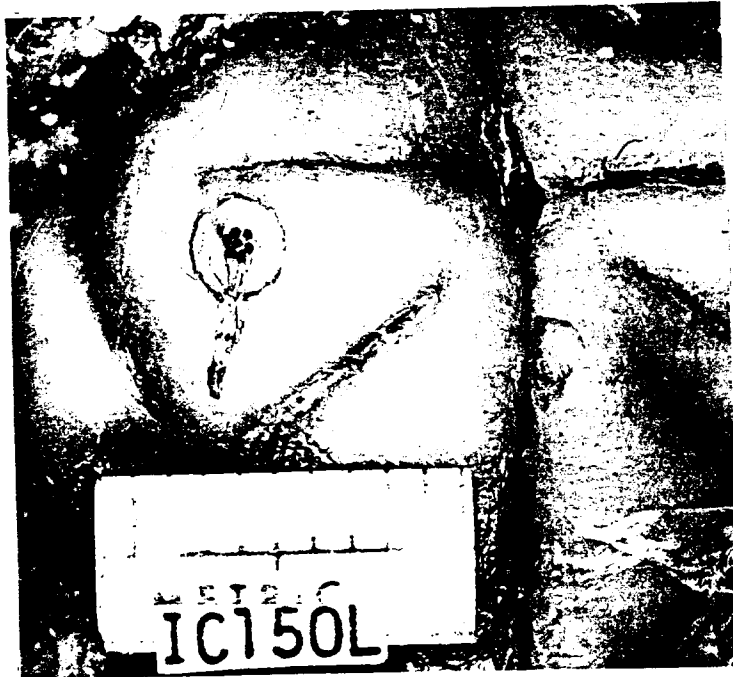
Fig. 1. Animal IC-150. Autopsy view of a 7-microelectrode array and a short segment of the electrode cables in situ in the left postcruciate gyrus. An accurate record of the angle between the cables and the cruciate sulcus enables identification of all microelectrode tracks. In this instance, electrode #'s 4 and 5 are most anterior, with #4 situated lateral to #5.
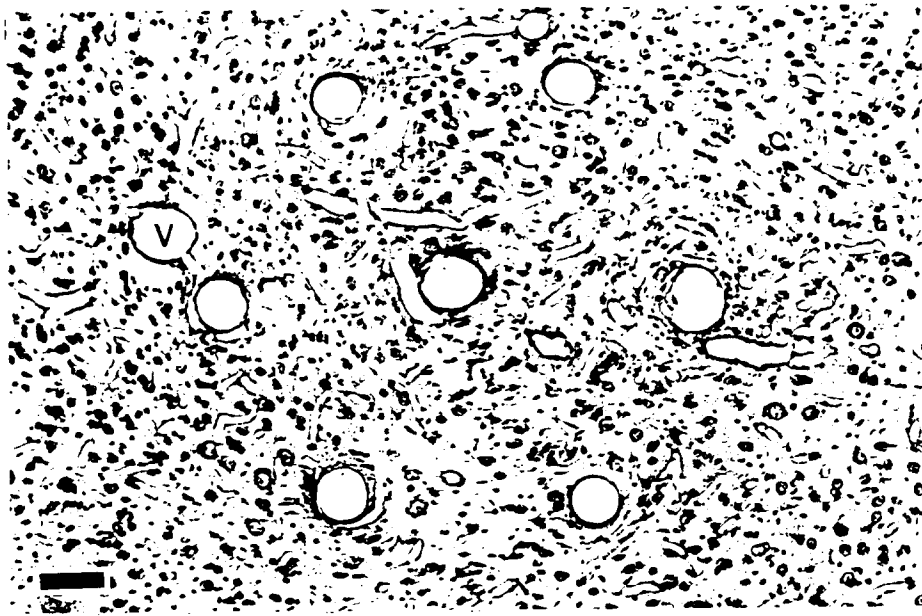
Fig. 2. Transverse section through the 7 tracks left by the array seen in Fig. 1. The depth is 300 µm below the pia. All tracks are surrounded by delicate connective tissue sheaths. There is mild vascular hypertrophy between the electrodes. V = blood vessel. H&E stain. Bar = 100 µm. This and all succeeding sections were cut horizontally through the electrode sites.
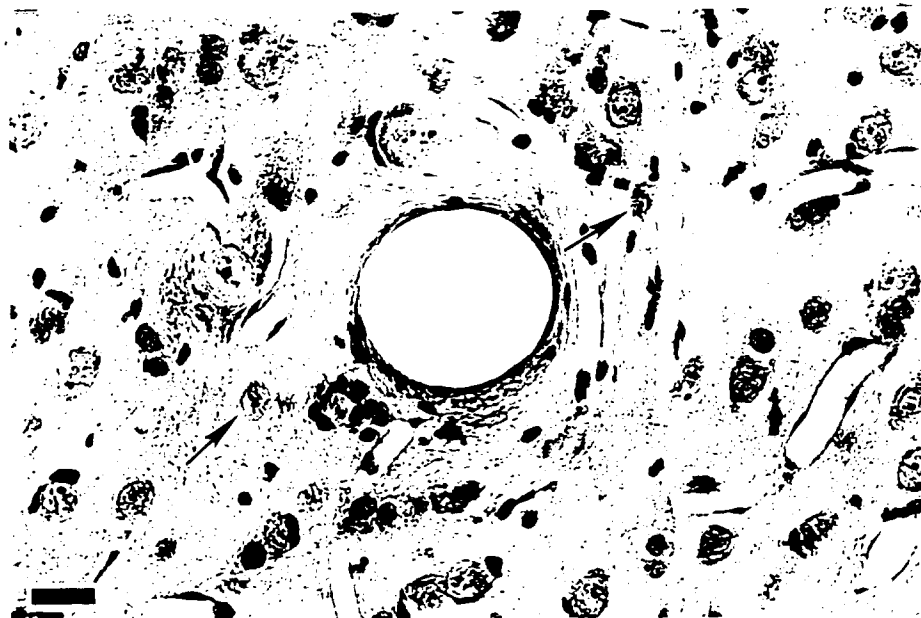
Fig. 3. Higher magnification of one of the microelectrode tracks seen in Fig. 2. Nearby neurons (arrows) and blood vessels appear normal . Bar = 25 µm.
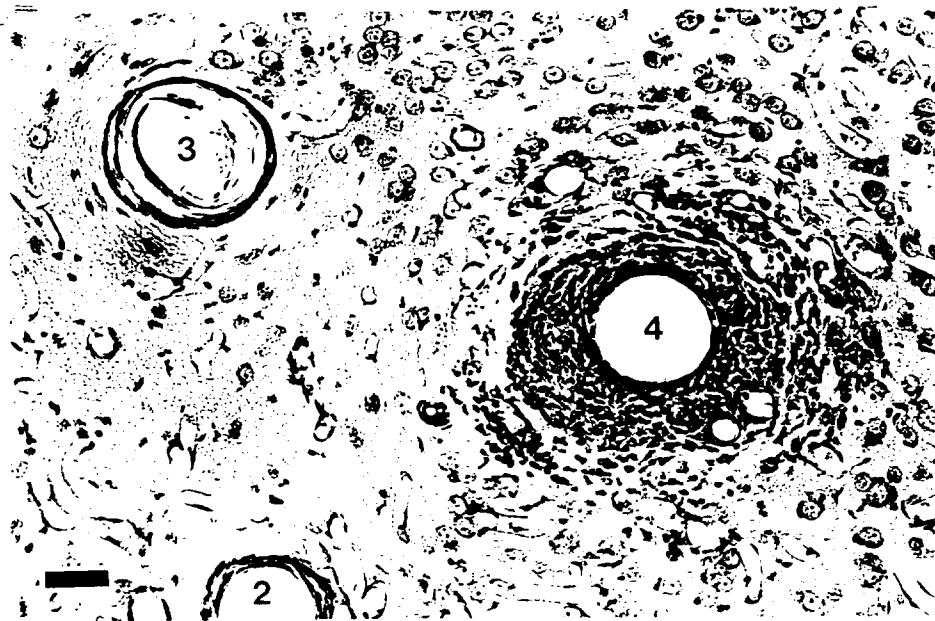
Fig. 4. Animal IC-150. The section is at a depth of 70 μm below the pia. Aside from some fraying of the connective tissue sheath around the tracks, electrode tracks #2 (2) and #3 (3) and adjacent neuropil appear normal. Track #4 (4) is surrounded by a compact aggregate of glial cells having a total width of about 26 μm. Neurons at the periphery of the aggregate appear normal. This is the closest point to the pia (70 μm) at which we observed gliosis in the series of animals. Nissl Stain. Bar = 50 μm.
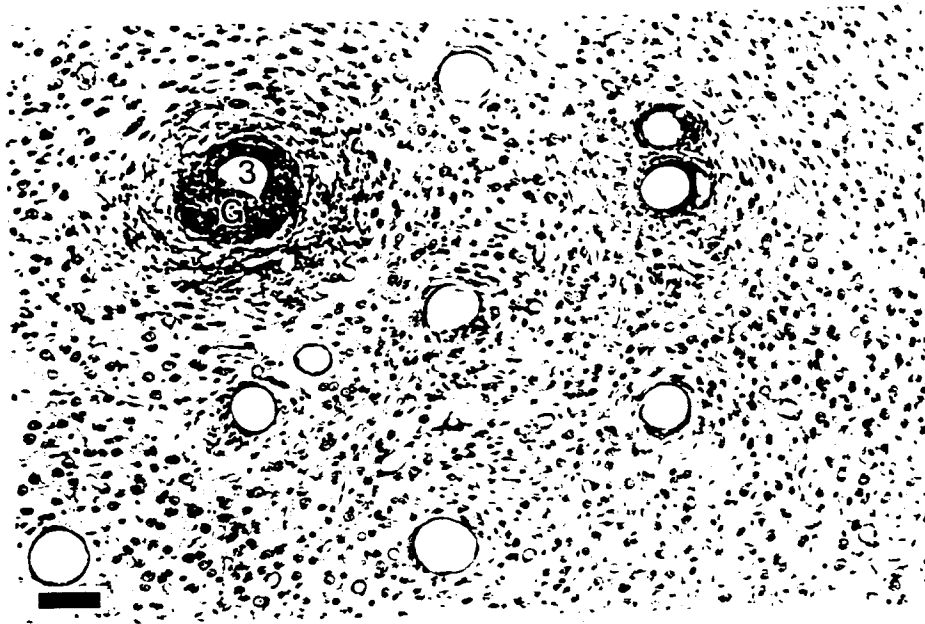
Fig. 5. Animal, IC-149. A section at a depth of 210 μm. Marked gliosis (G) surrounds electrode track #3 (3). This is in marked contrast to the remaining portions of the track, which is lined by a delicate, thin sheath. H&E Stain. Bar = 100 μm.
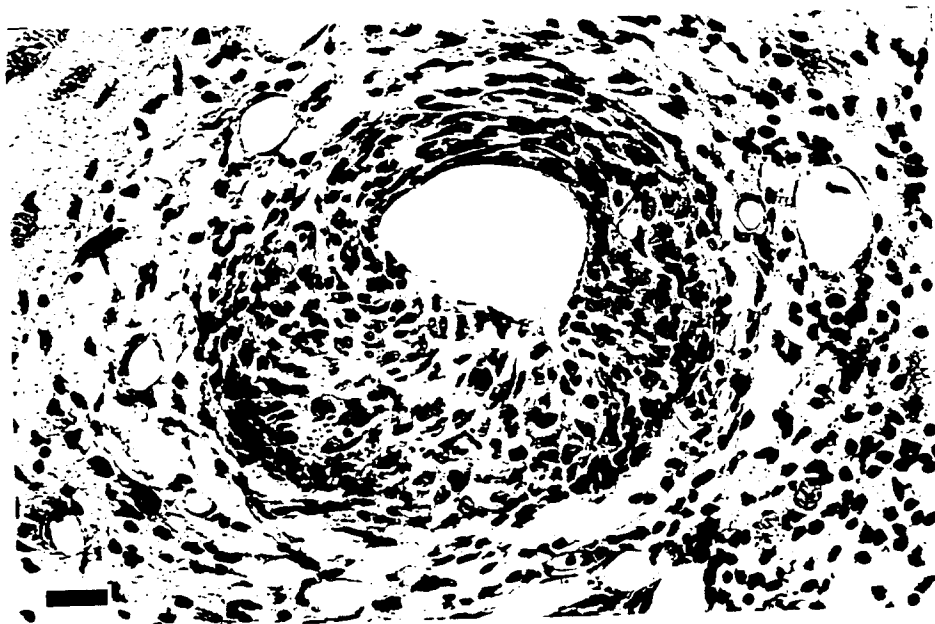
Fig. 6. Higher magnification of the gliotic accumulation around electrode track #3 shown in Fig. 4. Neither a glial nor connective tissue sheath had formed around the track. Numerous, widely separated astrocytes appear to be converging around the track. H&E Stain. Bar = 25 μm.
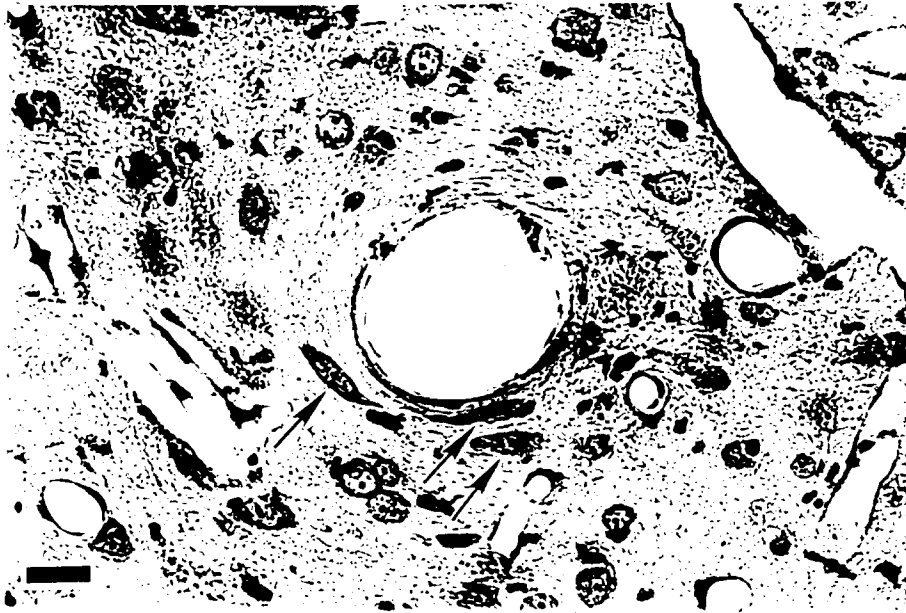
Fig. 7. IC-149. Three distorted neurons (arrows) lie near the central (#1) electrode track, at a depth of 630 µm. Inasmuch as these neurons lie opposite to the insulated portion of the shaft and far from the site of the tip, this phenomenon is attributed to mechanical displacement of the tissue during electrode insertion. Nissl Stain. Bar = 25 µm.
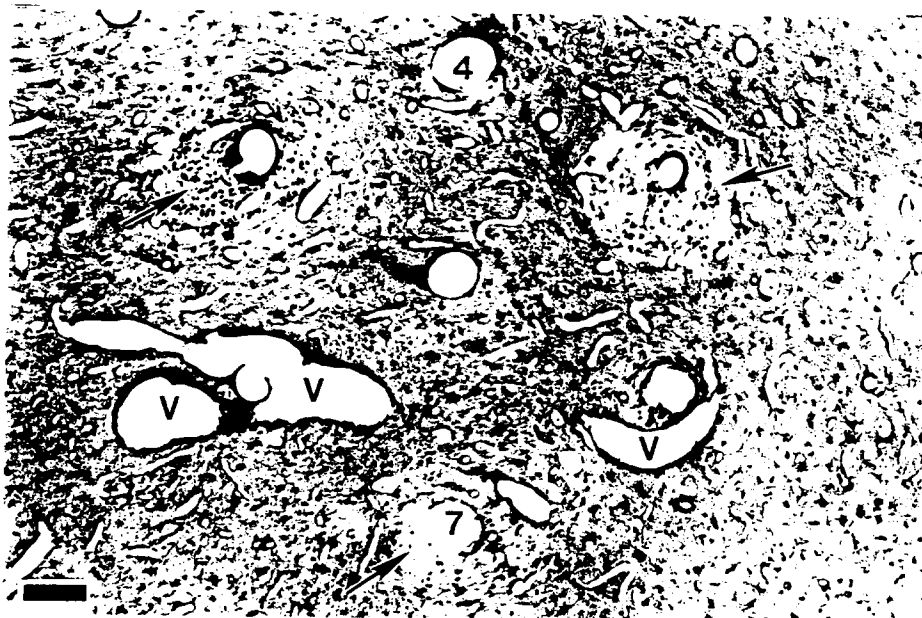
Fig. 8. IC-149. Depth 600 µm. Three of the 7 microelectrode tracks are surrounded by marked edema (arrows) and slight gliosis. Prominent vascular hypertrophy (V) accompanies two of the tracks. Although edema was present at several locations along the several shafts, it was almost never present at the sites of the microelectrode tips. Vascular hypertrophy or hyperplasia at various levels were a common occurrence in this series of animals. Masson's stain. Bar= 100 µm.
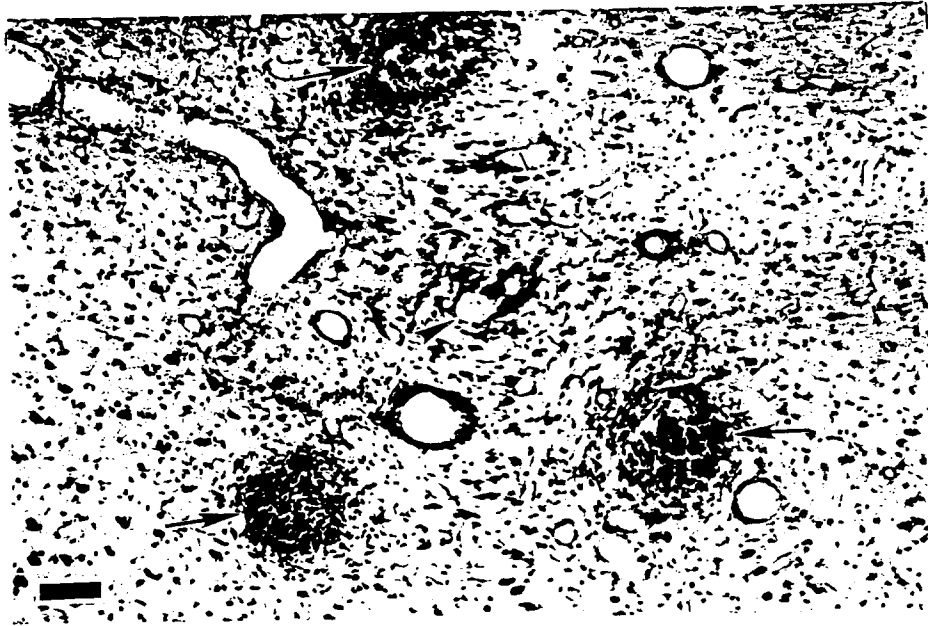
Fig. 9. IC-153. Depth 880 µm. There are dense lymphocytic accumulations at 3 of the 5 pulsed electrode tip sites (arrows). The unpulsed electrode #1 in the center of the array (arrow head) did not show this phenomenon at any level. H&E stain. Bar = 100 µm.
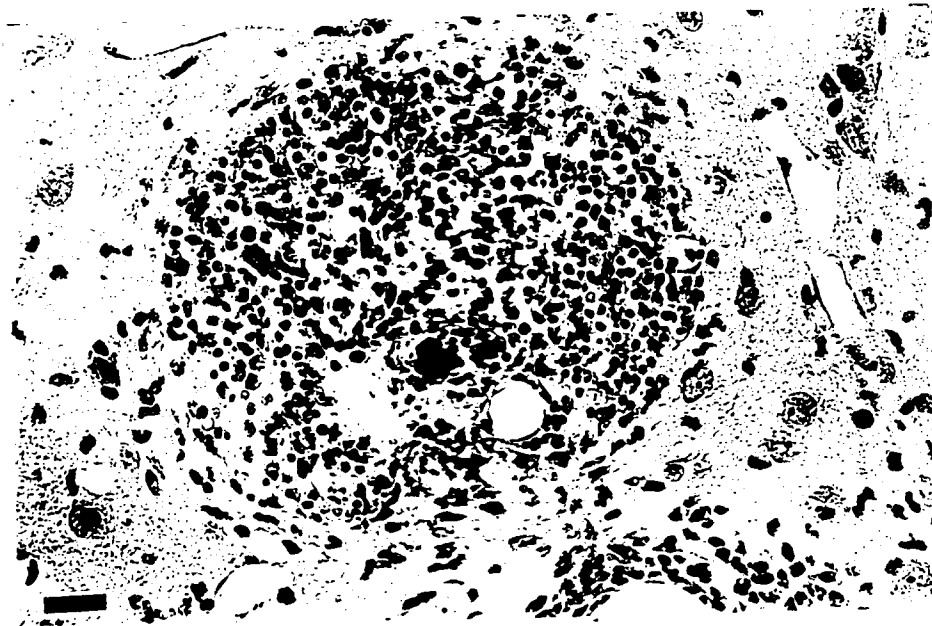

Fig. 10. IC-153. Depth 680 µm. This site of the tip of a pulsed microelectrode (#2) was 200 µm above the sites of the 3 tips shown in Fig. 9. The sites of all 5 pulsed tips were surrounded by aggregates of lymphocytes. H&E Stain. Bar = 25 µm.
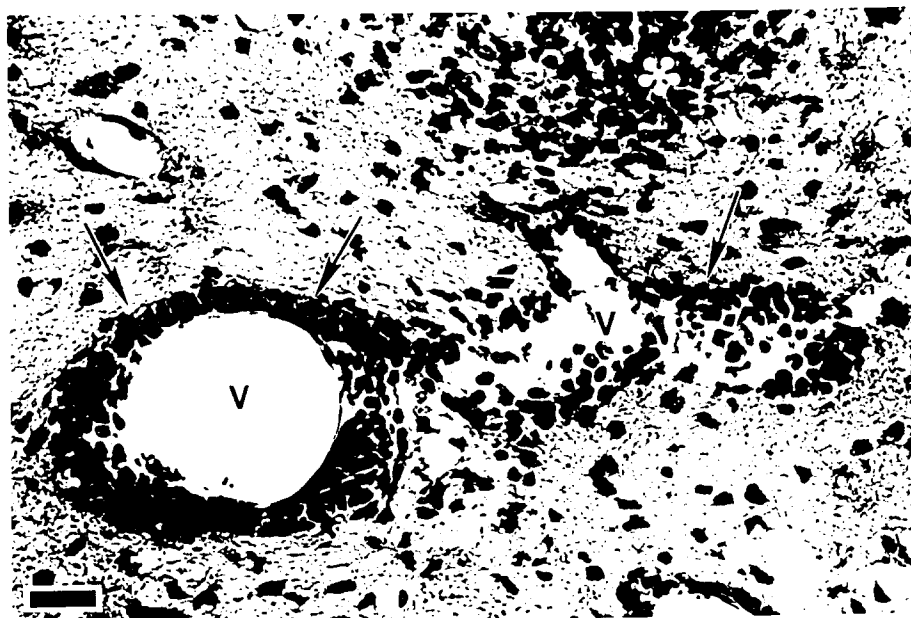
Fig. 11. IC-153. Blood vessel (V) near a microelectrode track, showing marked lymphocyte cuffing (arrows) and migration of the lymphocytes toward a pulsed electrode site (*). H&E stain. Bar = 25 μm.
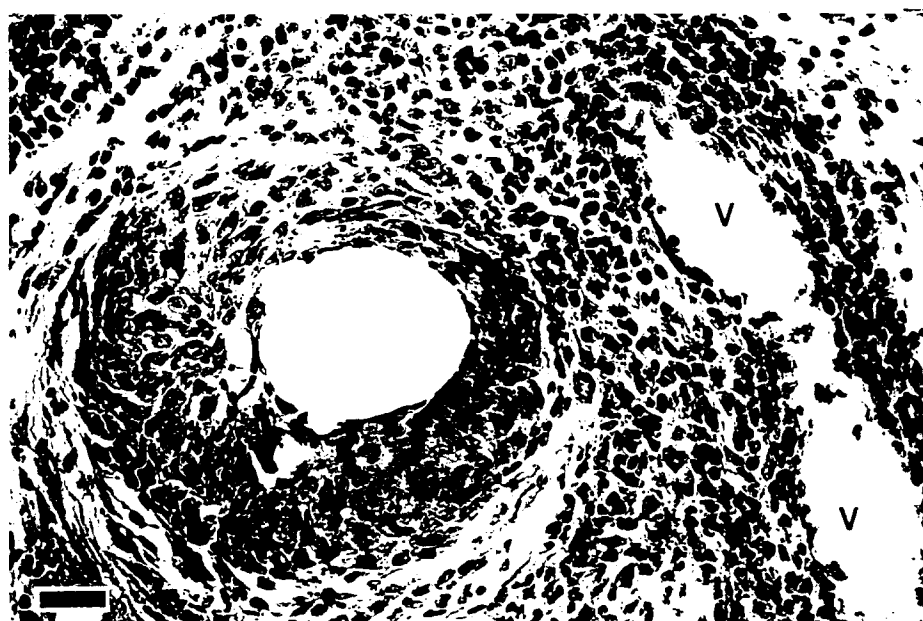

Fig. 12. IC-150. Packed glial cells surrounding the track of electrode #7 (7), the only pulsed electrode in the array. Lymphocytes were streaming from a nearby blood vessel (V), apparently towards the pulsed electrode site, and skirting the mass of glia cells. Nissl stain. Bar = 25 μm.